

## Interlayer $\Gamma$ - $X$ scattering in staggered-alignment $\text{Al}_{0.34}\text{Ga}_{0.66}\text{As}$ -AlAs ternary alloy multiple-quantum-well structures

Yasuaki Masumoto, Tomobumi Mishina, Fumio Sasaki, and Mitsuhiro Adachi

*Institute of Physics, University of Tsukuba, Tsukuba, Ibaraki 305, Japan*

(Received 26 June 1989)

The interlayer  $\Gamma$ - $X$  scattering rate of photoexcited electrons was measured in staggered-alignment  $\text{Al}_{0.34}\text{Ga}_{0.66}\text{As}$ -AlAs ternary alloy multiple-quantum-well structures. The scattering process was directly probed by femtosecond pump-and-probe spectroscopy. The mean  $\Gamma$ - $X$  scattering time of electrons across the interface between  $\text{Al}_{0.34}\text{Ga}_{0.66}\text{As}$  layers and AlAs layers at 4.2 K is determined to be 1.2 ps, which is longer than that observed recently in GaAs-AlAs short-period superlattices and is 20 times longer than that observed in bulk GaAs at 295 K. The slowing mechanism is ascribed to the small penetration of the evanescent  $\Gamma$  electrons into the AlAs barrier layers.

The recent femtosecond spectroscopy has opened the possibility to explore the ultrafast relaxation processes of photoexcited carriers in semiconductors. Especially, ultrafast intervalley scattering of photoexcited electrons in bulk semiconductors, GaAs and  $\text{Al}_x\text{Ga}_{1-x}\text{As}$ , was investigated by the state-of-the-art laser technology.<sup>1-4</sup> One of the next targets of the ultrafast laser technology is to extend its versatility to a variety of materials and to explore new physics. In this work, we investigated the interlayer  $\Gamma$ - $X$  scattering processes of electrons in staggered-alignment  $\text{Al}_{0.34}\text{Ga}_{0.66}\text{As}$ -AlAs ternary alloy multiple-quantum-well structures. In  $\text{Al}_x\text{Ga}_{1-x}\text{As}$ -AlAs ternary alloy multiple-quantum-well structures, the  $\Gamma$  electron state in the  $\text{Al}_x\text{Ga}_{1-x}\text{As}$  well layer crosses the  $X$  electron state in the AlAs layer at a certain value of  $x$ .<sup>5-8</sup> When the  $\text{Al}_x\text{Ga}_{1-x}\text{As}$  layer thickness is 10 nm, the crossover was expected to occur at the Al composition of 0.2 and was verified experimentally.<sup>8</sup> Around the  $\Gamma$ - $X$  crossover, interlayer  $\Gamma$ - $X$  scattering processes are expected to occur. Therefore, we can study dynamically the interlayer  $\Gamma$ - $X$  scattering processes of electrons by measuring the temporal change of the number of photogenerated  $\Gamma$  electrons in  $\text{Al}_x\text{Ga}_{1-x}\text{As}$  layers around the  $\Gamma$ - $X$  crossover. The measured results are compared with the very recent work by Feldmann *et al.* which studied the interlayer  $\Gamma$ - $X$  scattering processes of electrons in GaAs-AlAs short-period superlattices.<sup>9</sup>

In this work, two samples were mainly investigated. One is 100 alternate layers of 11.8 nm  $\text{Al}_{0.12}\text{Ga}_{0.88}\text{As}$  and 4.2 nm AlAs. The other is 100 alternate layers of 9.2 nm  $\text{Al}_{0.34}\text{Ga}_{0.66}\text{As}$  and 2.7 nm AlAs. Two subsidiary samples, 100 alternate layers of 9.6 nm GaAs and 9.1 nm AlAs and those of 9.6 nm  $\text{Al}_{0.41}\text{Ga}_{0.59}\text{As}$  and 2.8 nm AlAs, were also used to ascertain the phenomena. The luminescence and nonlinear absorption study of them were already reported by one of us.<sup>8</sup> The study informed us of the band-offset ratio and the relevant energy levels for our samples. Energy-level diagrams corresponding to two samples are schematically shown in Fig. 1. Two samples are representatives situated at both the sides of the interlayer  $\Gamma$ - $X$  crossover. In the sample  $\text{Al}_{0.12}\text{Ga}_{0.88}\text{As}$ -AlAs, the  $\Gamma$  electron state in the  $\text{Al}_{0.12}\text{Ga}_{0.88}\text{As}$  layer is lower than the  $X$ ,

$L$ , and  $\Gamma$  electron states in the AlAs layer. The sample is a nested-alignment, type-I, multiple-quantum-well structure. In the  $\text{Al}_{0.34}\text{Ga}_{0.66}\text{As}$ -AlAs sample, on the other hand, the  $X$  electron state in the AlAs layer is lower than the  $\Gamma$  electron state in the  $\text{Al}_{0.34}\text{Ga}_{0.66}\text{As}$  layer. The sample is a staggered-alignment, staggered type-II, multiple-quantum-well structure. In fact, the sample shows two distinct luminescence peaks,  $\Gamma$ - $\Gamma$  and  $X$ - $\Gamma$  recombination peaks, at low temperatures.<sup>8</sup> Comparing the two samples, the additional relaxation path, the interlayer transfer of  $\Gamma$  electron in the  $\text{Al}_{0.34}\text{Ga}_{0.66}\text{As}$  layer to the  $X$  state in the AlAs layer, is expected for the electrons at the bottom of the wells in the sample  $\text{Al}_{0.34}\text{Ga}_{0.66}\text{As}$ -AlAs but not in the sample  $\text{Al}_{0.12}\text{Ga}_{0.88}\text{As}$ -AlAs. Therefore, our experiments are motivated to clarify the difference in dynamics of photoexcited electrons in the two samples and the mechanism of the interlayer  $\Gamma$ - $X$  intervalley scattering.

Samples directly immersed in liquid helium or liquid nitrogen were investigated. The experiment was performed using the femtosecond pump-and-probe spectrometer developed by us. The laser system was composed of a cw mode-locked Nd<sup>3+</sup>:YAG laser, the first-stage pulse compressor, a second-harmonic generator, a synchronously pumped cavity-dumped dye laser, the second-stage pulse compressor, and a dye amplifier pumped by a  $Q$ -

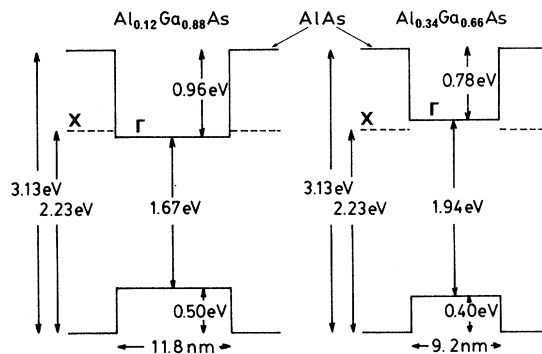


FIG. 1. Schematic energy diagrams for two samples, type-I  $\text{Al}_{0.12}\text{Ga}_{0.88}\text{As}$ -AlAs and staggered type-II  $\text{Al}_{0.34}\text{Ga}_{0.66}\text{As}$ -AlAs.

switched Nd<sup>3+</sup>:YAG laser. The power of the laser pulses (583 nm) was 400  $\mu\text{J}$  with the pulse duration of 260 fs, which easily generates white continuum pulses. Pump-and-probe experiments were performed by using 583-nm pump pulses going through an optical delay and white-continuum pulses. Pump pulses (583 nm) hit the sample with a power density of 700  $\mu\text{J}/\text{cm}^2$ . The white-continuum probe pulses transmitted through the center of the pumped region of the sample were spectrally analyzed by a 25-cm monochromator, an optical multiple-channel analyzer, and a computer. The temporal change of the absorption was observed by the monochromator, a photomultiplier, and a boxcar integrator with the variation of the optical delay controlled by the computer.

In the inset of Figs. 2 and 3, the absorption spectra around the lowest-energy heavy-exciton resonance ( $\Gamma$ - $\Gamma$ ,  $n=1$ ) are shown. As is shown, the exciton structure is clearly observed without the pump. However, the structure is bleached under the pump. The temporal change of the absorption coefficient  $-\Delta\alpha$  around the lowest energy exciton resonance for two samples at 4.2 K are plotted in Figs. 2 and 3, respectively. In the sample  $\text{Al}_{0.12}\text{Ga}_{0.88}\text{As}-\text{AlAs}$ ,  $-\Delta\alpha$  rises at a time constant of 1.7 ps, and then is kept constant. The similar monotonous rise was also observed at the lowest energy exciton resonance in the sample  $\text{GaAs}-\text{AlAs}$ . In the sample  $\text{Al}_{0.34}\text{Ga}_{0.66}\text{As}-\text{AlAs}$ , on the other hand,  $-\Delta\alpha$  rises at a time of 1.2 ps, and then decreases at a fast decay time of 1.2 ps with a successive constant tail. The constant tail remains until 400 ps. The fitting is a convoluted result with the convolution of squares of sech functions, where the half width of the convolution is 400 fs. The results were not altered even at 77 K. The temporal change is the same for the lowest energy light exciton resonance. Similar characteristics—fast rise and successive fast recovery (1.0 ps) in the time-resolved absorption—were also observed in another sample of  $\text{Al}_{0.41}\text{Ga}_{0.59}\text{As}-\text{AlAs}$  at 77 K. This observation is similar

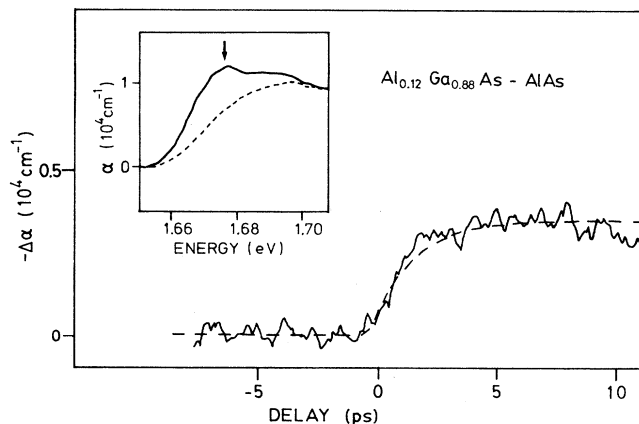


FIG. 2. Temporal change of the absorption change of the lowest heavy excitons denoted by an arrow in the  $\text{Al}_{0.12}\text{Ga}_{0.88}\text{As}-\text{AlAs}$  sample. The dashed line shows the fitting by  $1 - \exp(-t/\tau_r)$  convoluted by the convolution of the laser pulse shape, where  $\tau_r = 1.7$  ps. In the inset the absorption spectra with and without pump pulses are shown by dashed and solid lines, respectively.

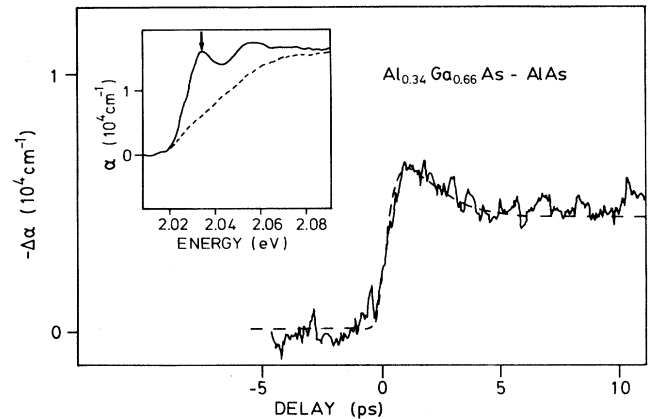


FIG. 3. Temporal change of the absorption change of the lowest heavy excitons denoted by an arrow in the  $\text{Al}_{0.34}\text{Ga}_{0.66}\text{As}-\text{AlAs}$  sample. The dashed line shows the fitting by  $[1 - \exp(-t/\tau_r)][\exp(-t/\tau_d) + c]$  convoluted by the convolution of the laser pulse shape, where  $\tau_r = 1.2$  ps,  $\tau_d = 1.2$  ps, and  $c = 0.29$ . In the inset the absorption spectra with and without pump pulses are shown by dashed and solid lines, respectively.

to the results by Becker *et al.*, if the time scale of their result is expanded by about 2 orders of magnitude. It is also similar to the results by Feldmann *et al.*, although the fast recovery time in our results is longer than that in their results.

Here, we must note the mechanism of the exciton bleaching and what the bleaching intensity stands for. In our experimental situation, the band-to-band excitation at 4.2 K, the exciton bleaching is considered to occur dominantly as a result of phase-space filling and exchange effects.<sup>10,11</sup> Therefore, the bleaching intensity is mostly proportional to the  $\Gamma$  electron population at the bottom of the well. The Coulomb screening by the electron-hole plasma may work also to reduce the exciton absorption in our experiments. Even if plasma screening works together, the reduction of the exciton absorption is expected to be proportional to the electron-hole plasma density, that is, the  $\Gamma$  electron density. Therefore, the decrease in the exciton absorption represents the  $\Gamma$  electron population.

In the sample  $\text{Al}_{0.34}\text{Ga}_{0.66}\text{As}-\text{AlAs}$ , the  $\Gamma$  electron state in  $\text{Al}_{0.34}\text{Ga}_{0.66}\text{As}$  is higher than the  $X$  electron state in  $\text{AlAs}$  by 100 meV. Therefore, the interlayer transfer of the  $\Gamma$  electrons in the  $\text{Al}_{0.34}\text{Ga}_{0.66}\text{As}$  layer to the  $X$  electron state in the  $\text{AlAs}$  layer is possible. We estimated the interlayer relaxation rate by the penetration of the  $\Gamma$  electron wave function to the  $\text{AlAs}$  layer and the  $\Gamma$ - $X$  scattering rate of electrons in  $\text{AlAs}$ , as shown in the next paragraph. Fortunately, the  $\Gamma$ - $X$  phonon scattering rate of electrons in  $\text{GaAs}$  has been a current target of the state-of-the-art ultrafast laser spectroscopy.<sup>1-4</sup> The mean  $\Gamma$ - $X$  scattering time of electrons in  $\text{GaAs}$  was measured to be 55 fs at 295 K by the femtosecond pump-and-probe spectroscopy.<sup>4</sup> The time almost agrees with the calculated one on the model of the intervalley scattering with the emission and absorption of optical phonons.<sup>1</sup> The scattering rate is governed by the deformation potential. Because the deformation potential of  $\text{AlAs}$  is not known, the  $\Gamma$ - $X$

scattering rate of electrons in AlAs is assumed to be equal to that in GaAs.<sup>12</sup>

To interpret our observation, we estimated the interlayer  $\Gamma$ - $X$  transfer rate by the simplest method described below. The penetration of the  $\Gamma$  electron wave function to the AlAs layer,  $P_\Gamma$ , is estimated by the envelope-function approximation of Bastard.<sup>13</sup> We solved the effective-mass equation

$$[-\hbar^2 \nabla^2 / 2m^*(z) - E - V(z)]F(z) = 0,$$

where  $z$  is the direction of superlattice growth,  $F(z)$  is the envelope function,  $V(z)$  the potential profile, and  $m^*(z)$  the electron effective mass. The boundary conditions are given by the continuity of both  $F(z)$  and  $1/m^*(z) \times (\partial F / \partial z)$ . Numerical calculations for  $\text{Al}_{0.34}\text{Ga}_{0.66}\text{As}$ -AlAs were carried out with the following parameters, the electron effective mass in  $\text{Al}_{0.34}\text{Ga}_{0.66}\text{As}$   $0.095m_0$ , that in AlAs  $0.15m_0$ , the potential-energy gap  $0.783$  eV and the well width  $9.2$  nm.<sup>8,12,14</sup> The potential-energy gaps for our samples were determined by the band offset ratio of  $0.66:0.34$  obtained experimentally.<sup>8</sup> The estimated penetration probability of the  $\Gamma$  electrons,  $P_\Gamma$ , that is the square of the evanescent  $\Gamma$  wave function in the AlAs layer is  $0.68\%$  of the total. The small value of  $P_\Gamma$  comes from the fairly large thickness of GaAs layers,  $9.2$  nm, which prevents the miniband formation. The interlayer  $\Gamma$ - $X$  scattering rate is estimated by the  $\Gamma$ - $X$  scattering rate in AlAs divided by the probability of the  $\Gamma$  electron wave function in AlAs. Thus, the mean interlayer  $\Gamma$ - $X$  scattering time is estimated to be  $4.9$  ps by dividing  $55$  fs by  $0.0068$  and the ratio of the phonon factor  $[2N(295) + 1] / [2N(4.2) + 1] = 1.66$ , where  $N(T)$  is the longitudinal-optical-phonon occupation number at temperature  $T$ . The observed fast decay time of the exciton population agrees with the estimation within an order of magnitude.

The penetration probability of the  $\Gamma$  electrons in the AlAs layer,  $P_\Gamma$ , and those of the  $X_z$  and  $X_{x,y}$  electrons in the  $\text{Al}_x\text{Ga}_{1-x}\text{As}$  or GaAs layer,  $P_X$ , for our samples,  $\text{Al}_{0.34}\text{Ga}_{0.66}\text{As}$ -AlAs and  $\text{Al}_{0.41}\text{Ga}_{0.59}\text{As}$ -AlAs, and samples studied by Feldman *et al.* are listed in Table I. These values were calculated in the same way as described in the preceding paragraph. The calculated values on the basis of the Kronig-Penney model are also listed.<sup>9,15</sup> Table I shows that the essential difference between our samples and samples studied by Feldmann *et al.* lies in the values of  $P_\Gamma$  which comes from the difference in the well layer thickness. Comparing the penetration probability of the wave functions and the fast recovery time constant  $\tau_d$  observed in the pump-and-probe spectroscopy, we can find a correlation between  $P_\Gamma$  and  $\tau_d$  but cannot between  $P_X$  and  $\tau_d$ . Therefore, the observed results strongly suggest that the interlayer  $\Gamma$ - $X$  scattering is dominated by the penetration of the evanescent  $\Gamma$  electrons into the AlAs layers. Although the envelope-function approximation is simplest, we believe that it well describes the real situation at the interface. The more sophisticated calculation, for example, that on the basis of the interface matrix approach may be useful for the better understanding of the interlayer  $\Gamma$ - $X$  intervalley scattering.<sup>16</sup>

TABLE I. The penetration probability of the  $\Gamma$  electrons in the AlAs layer  $P_\Gamma$ , those of the  $X_z$  and  $X_{x,y}$  electrons in the  $\text{Al}_x\text{Ga}_{1-x}\text{As}$  or GaAs layer  $P_X$ , and the fast recovery time constant  $\tau_d$  observed in the pump-and-probe experiments. Probabilities in the upper column are values calculated on the procedures described in the text. Probabilities in the lower column are values calculated on the Kronig-Penney model (Refs. 9 and 15).

|  | $P_\Gamma$     | $X_z$           | $X_{x,y}$     | $\tau_d$            |
|--|----------------|-----------------|---------------|---------------------|
| $\text{Al}_{0.34}\text{Ga}_{0.66}\text{As}$ -AlAs<br>9.2 nm 2.7 nm | 0.68%<br>0.75% | 1.5%<br>3.0%    | 9.0%<br>18%   | 1.2 ps              |
| $\text{Al}_{0.41}\text{Ga}_{0.59}\text{As}$ -AlAs<br>9.6 nm 2.8 nm | 0.62%<br>0.68% | 1.5%<br>3.0%    | 8.9%<br>18%   | 1.0 ps <sup>a</sup> |
| GaAs-AlAs<br>2.55 nm 2.55 nm                                       | 10.6%<br>12%   | 1.2%<br>2.4%    | 7.4%<br>18%   | 130 fs <sup>b</sup> |
| GaAs-AlAs<br>3.11 nm 6.79 nm                                       | 7.6%<br>7.5%   | 0.097%<br>0.25% | 0.94%<br>2.1% | 620 fs <sup>b</sup> |

<sup>a</sup>Measured value at 77 K.

<sup>b</sup>Reference 9.

Comparing our results with those of the preceding authors who investigated the ultrafast intervalley scattering,<sup>1-4</sup> we can fully understand the rise as well as decay of the exciton bleaching in two samples. In the sample  $\text{Al}_{0.12}\text{Ga}_{0.88}\text{As}$ -AlAs, the  $X$  and  $L$  electron states in  $\text{Al}_{0.12}\text{Ga}_{0.88}\text{As}$  are higher than the  $\Gamma$  electron state in  $\text{Al}_{0.12}\text{Ga}_{0.88}\text{As}$  by  $0.34$  and  $0.21$  eV, respectively. The  $X$  electron state in AlAs is higher than the  $\Gamma$  electron state in  $\text{Al}_{0.12}\text{Ga}_{0.88}\text{As}$  by  $0.06$  eV. The pump laser energy is  $2.12$  eV which is higher than the  $X$  electron state in  $\text{Al}_{0.12}\text{Ga}_{0.88}\text{As}$  by  $0.1$  eV. Therefore, the electron-electron scattering, Fröhlich-type LO-phonon scattering,  $\Gamma$ - $X$ ,  $\Gamma$ - $L$ ,  $\Gamma$ - $X$ - $\Gamma$ , and  $\Gamma$ - $L$ - $\Gamma$  intervalley scattering takes place frequently in the  $\text{Al}_{0.12}\text{Ga}_{0.88}\text{As}$  layer. The intervalley scattering mechanism works to slow down the cooling of  $\Gamma$  electron temperature. Because the exciton bleaching is proportional to the  $\Gamma$  electron population at the bottom of the well, the rise of the exciton bleaching at a time constant of  $1.7$  ps is understood consistently with the results by Shah *et al.*<sup>3</sup> Then, the electron population slowly decreases as a result of the competition between the electron cooling and the radiative and nonradiative annihilations. In the sample  $\text{Al}_{0.34}\text{Ga}_{0.66}\text{As}$ -AlAs, on the other hand, the  $X$  electron state in AlAs is lower than the  $\Gamma$  electron state in  $\text{Al}_{0.34}\text{Ga}_{0.66}\text{As}$  by  $0.12$  eV. The  $X$  and  $L$  electron states in the  $\text{Al}_{0.34}\text{Ga}_{0.66}\text{As}$  layer is higher than the  $\Gamma$  electron state in the  $\text{Al}_{0.34}\text{Ga}_{0.66}\text{As}$  layer by  $0.111$  and  $0.078$  eV, respectively. The pump laser is higher than the  $\Gamma$ ,  $L$ , and  $X$  states in the  $\text{Al}_{0.34}\text{Ga}_{0.66}\text{As}$  layer. Therefore, the intervalley scattering also works. However, the additional decay channel of the electron population, interlayer  $\Gamma$ - $X$  scattering, arises. This additional decay process contributes the  $1.2$ -ps decay of the electron population at the bottom of the well. The slow tail part comes from the cooling

of the electron system.

In summary, we observed the interlayer  $\Gamma$ - $X$  scattering of electrons in the staggered-alignment  $\text{Al}_{0.34}\text{Ga}_{0.66}\text{As}$ -AlAs ternary alloy multiple-quantum-well structures. The interlayer  $\Gamma$ - $X$  scattering time was determined to be 1.2 ps by the femtosecond pump-and-probe experiments. The scattering rate is explained by taking account of the  $\Gamma$ - $X$  intervalley scattering rate and the penetration of the  $\Gamma$  electron wave function into AlAs layers.

The authors wish to thank Dr. H. Iwamura at Nippon Telegraph and Telephone Corporation for providing high-quality samples. They also wish to thank Professor M. Matsuura at Yamaguchi University for valuable discussions. This work was supported in part by the Scientific Research Grant-in-Aid No. 01604515 for the Scientific Research on Priority Areas, New Functionality Materials-Design, Preparation and Control-by the Ministry of Education, Science and Culture of Japan.

- 
- <sup>1</sup>A. J. Taylor, D. J. Erskin, and C. L. Tang, *J. Opt. Soc. Am. B* **2**, 663 (1985).  
<sup>2</sup>R. W. Schoenlein, W. Z. Lin, E. P. Ippen, and J. G. Fujimoto, *Appl. Phys. Lett.* **51**, 1442 (1987).  
<sup>3</sup>J. Shah, B. Deveaud, T. C. Damen, W. T. Tsang, A. C. Gos-sard, and P. Lugli, *Phys. Rev. Lett.* **59**, 2222 (1987).  
<sup>4</sup>P. C. Becker, H. L. Fragnito, C. H. Brito Cruz, J. Shah, R. L. Fork, J. E. Cunningham, J. E. Henry, and C. V. Shank, *Appl. Phys. Lett.* **53**, 2089 (1988).  
<sup>5</sup>B. A. Wilson, P. Dawson, C. W. Tu, and R. C. Miller, *J. Vac. Sci. Technol. B* **4**, 1037 (1986).  
<sup>6</sup>P. Dawson, B. A. Wilson, C. W. Tu, and R. C. Miller, *Appl. Phys. Lett.* **48**, 541 (1986).  
<sup>7</sup>For a review of staggered-alignment multiple-quantum-well structures, see B. A. Wilson, *IEEE J. Quantum Electron QE-24*, 1763 (1988).  
<sup>8</sup>Y. Masumoto and T. Tsuchiya, *J. Phys. Soc. Jpn.* **57**, 4403 (1988).  
<sup>9</sup>J. Feldmann, R. Sattmann, E. O. Göbel, J. Kuhl, J. Hebling, K. Ploog, R. Muralidharan, P. Dawson, and C. T. Foxon, *Phys. Rev. Lett.* **62**, 1892 (1989).  
<sup>10</sup>W. H. Knox, C. Hirlimann, D. A. B. Miller, J. Shah, D. S. Chemla, and C. V. Shank, *Phys. Rev. Lett.* **56**, 1191 (1986).  
<sup>11</sup>D. S. Chemla, D. A. B. Miller, and S. Schmitt-Rink, in *Optical Nonlinearities in Semiconductors*, edited by H. Haug (Academic, Boston, 1988), Chap. 4.  
<sup>12</sup>S. Adachi, *J. Appl. Phys.* **58**, R1 (1985).  
<sup>13</sup>G. Bastard, *Phys. Rev. B* **24**, 5693 (1981).  
<sup>14</sup>H. C. Casey, Jr. and M. B. Panish, *Heterostructure Lasers* (Academic, New York, 1978), Chap. 4.  
<sup>15</sup>H.-S. Cho and P. R. Prucnal, *Phys. Rev. B* **36**, 3237 (1987).  
<sup>16</sup>T. Ando and H. Akera, in *Proceedings of the Nineteenth International Conference on the Physics of Semiconductors, Warsaw, Poland, 1988* (World Scientific, Singapore, in press).